# Multicomponent kinetic simulation of Bernstein–Greene–Kruskal modes associated with ion acoustic and dust-ion acoustic excitations in electron-ion and dusty plasmas

S. M. Hosseini Jenab and I. Kourakis

Citation: Physics of Plasmas (1994-present) **21**, 043701 (2014); doi: 10.1063/1.4869730
View online: http://dx.doi.org/10.1063/1.4869730
View Table of Contents: http://scitation.aip.org/content/aip/journal/pop/21/4?ver=pdfcov
Published by the AIP Publishing

# Multicomponent kinetic simulation of Bernstein–Greene–Kruskal modes associated with ion acoustic and dust-ion acoustic excitations in electron-ion and dusty plasmas

S. M. Hosseini Jenab[1,a)] and I. Kourakis[2,b)]
[1]*Department of Physics, South Tehran Branch, Islamic Azad University, Tehran, Iran*
[2]*Center for Plasma Physics, Department of Physics and Astronomy, Queen's University Belfast, Belfast BT7 1NN, Northern Ireland, United Kingdom*

(Received 21 October 2013; accepted 17 March 2014; published online 2 April 2014)

A series of numerical simulations based on a recurrence-free Vlasov kinetic algorithm presented earlier [Abbasi *et al.*, Phys. Rev. E **84**, 036702 (2011)] are reported. Electron-ion plasmas and three-component (electron-ion-dust) dusty, or complex, plasmas are considered, via independent simulations. Considering all plasma components modeled through a kinetic approach, the nonlinear behavior of ionic scale acoustic excitations is investigated. The focus is on Bernstein–Greene–Kruskal (BGK) modes generated during the simulations. In particular, we aim at investigating the parametric dependence of the characteristics of BGK structures, namely of their time periodicity $(\tau_{trap})$ and their amplitude, on the electron-to-ion temperature ratio and on the dust concentration. In electron-ion plasma, an exponential relation between $\tau_{trap}$ and the amplitude of BGK modes and the electron-to-ion temperature ratio is observed. It is argued that both characteristics, namely, the periodicity $\tau_{trap}$ and amplitude, are also related to the size of the phase-space vortex which is associated with BGK mode creation. In dusty plasmas, BGK modes characteristics appear to depend on the dust particle density linearly. © *2014 AIP Publishing LLC*. [http://dx.doi.org/10.1063/1.4869730]

## I. INTRODUCTION

Bernstein–Greene–Kruskal (BGK) modes are exact nonlinear stationary-profile solutions of the Vlasov–Poisson system of equations for collisionless and unmagnetized plasma, known to experience no Landau damping.[1] Such structures have been observed in laboratory experiments[2,3] and in space observations.[4–9] In 1965, O'Neil showed for the first time that nonlinear Landau damping results in the formation of oscillatory BGK modes.[10] These modes appear as excitations (disturbances) of the electric field envelope with characteristic timescale (periodicity) $(\tau_{trap})$ which is related to the particles' trapping and to their rotating motion. Particles trapped in potential wells associated with the propagating wave can be observed as a spinning vortex in the distribution function in phase space. Phase-space vortices are the fingerprints of trapped particles (and of BGK modes) and can be easily distinguished in phase space snapshots. The constant energy exchange between trapped particles and the wave leads to a fluctuating pattern in the electric field amplitude.[11,12] The occurrence of BGK modes depends on the relative strength between the amplitude oscillation period $\tau_{trap} = 2\pi\sqrt{m_e/eEk}$ (where $m_e$ and $e$ are the electron mass and charge, $E$ is the electric field amplitude, and $k$ is the wavenumber) and $\tau_L \simeq \gamma_L^{-1}$ (here, $\tau_L$ is the time scale associated to Landau damping, and $\gamma_L$ is the Landau damping rate).[10] If $\tau_{trap} \gg \tau_L$, no BGK modes are observed. In the opposite case, when $\tau_{trap} \leq \tau_L$, BGK modes occur. A one-dimensional (1D) geometry will be adopted throughout this work.

Our investigation relies on triggering an electrostatic excitation via an appropriate initial disturbance of the ion plasma species off equilibrium. The fundamental ion-scale electrostatic (ion-acoustic, IA) mode[11] consists of periodic oscillations of the inertial ion plasma species against an electron background which provides the necessary restoring force to sustain the oscillation. Interestingly, the presence of dust particulates in a so called *dusty plasma* was shown to lead, through the modification of the charge balance, to an increase of the IA wave phase speed. This has by now been identified as a new mode, termed the dust-ion acoustic wave (DIAW),[13] with a distinct frequency $\omega$ in the range $kv_{Td} \ll kv_{Ti} \ll \omega \ll kv_{Te}$ (where $v_{Ts}$ denotes the thermal velocity of species $s$ $(=d, i, e$ for dust, ions, or electrons, respectively). The nonlinear behavior of DIAWs has been considered in various theoretical papers; these excitations have recently been associated with BGK modes (dust-BGK mode, DBGK).[14]

The kinetic approach in computer simulation of the plasma behavior relies on the Vlasov[15] equation, in combination with Poisson's equation. A "splitting" kinetic simulation algorithm was proposed by Cheng and Knorr[16] while various improved methods have been introduced in recent years.[17–19] Although these simulation methods have provided valuable insight to plasma behavior, they all share a generic characteristic, in the form of a numerical error: Initial states of the distribution function will reappear in the simulation periodically (in around a recurrence time $t_r = 2\pi/(kdv)$ or its multiples, where $k$ is the wavenumber and $dv$ is the grid step in the

a)Email: mehdi.jenab@yahoo.com
b)Email: IoannisKourakisSci@gmail.com

 

velocity direction). This *recurrence effect*, which is entirely numerical and reflects no physical truth, makes the results of the simulation rather unreliable beyond time $t_r$. The recurrence effect has been waived in our simulation method[21] by adopting the algorithm proposed in Refs. 20; we refer the interested reader to that reference for details on the method.

Since BGK mode formation and particle trapping in general are highly nonlinear phenomena, these cannot be easily investigated through an analytical approach. Experimental results or computer simulations provide valuable insight in many questions arising in this area. Noteworthy is the work of Manfredi,[22] who showed that BGK modes associated with Langmuir waves in electron-ion plasmas are stable and thus, earlier analytical work[23,24] on decaying or unstable BGK modes should be revisited.

In the article at hand, the focus is on the parametric dependence of BGK modes on the electron-to-ion temperature ratio and, in the case of dusty plasma, on dust concentration. In an earlier paper,[25] linear IA and DIAWs have been studied through kinetic simulations and the dependence of the Landau damping rate $\gamma_l$ on relevant plasma parameters was investigated.[25] Noting that the question of the stability of one-hole BGK modes has not yet been answered exactly,[26] we will investigate here the first and the second peak of BGK modes, actually casting the focus on the short time development of nonlinear Landau damping.

The layout of this study goes as follows. In the Sec. II, we introduce the basic aspects of our theoretical model. In Sec. III, the results of a series of computer simulations for different parameters are presented and discussed. Section IV is dedicated to summarizing our results.

## II. MODEL AND NUMERICAL PROCEDURE

We consider a three-component plasma, consisting of electrons (mass $m_e$, charge $q_e = -e$), singly ionized ions (mass $m_i$, charge $q_i = +e$) and negatively charged dust (mass $m_d$, charge $q_d = -Z_d\, e$). Importantly, the dust charge will be assumed constant throughout this paper, i.e., dust charging mechanisms are neglected, actually a reasonable assumption at the (ionic) scale of interest. The presentation that follows proceeds by considering three plasma components, all appearing through the corresponding distribution function. In order to consider an "ordinary" electron-ion plasma, the dust component below will be formally "switched off" in the analysis, and also in the computer code. A one-dimensional (1D) Vlasov–Poisson system of equations will be adopted in our study.

Each plasma species is described by a Vlasov equation in the form

$$\frac{\partial f_s(x,v,t)}{\partial t} + v\frac{\partial f_s(x,v,t)}{\partial x} + \frac{q_s E(x,t)}{m_s} \times \frac{\partial f_s(x,v,t)}{\partial v} = 0, \quad s = e,i,d, \tag{1}$$

where $s = e, i, d$ denotes the corresponding plasma species in all algebraic expressions that follow; the variable $v$ denotes velocity in (1D) phase space.

The densities of the plasma components are given upon integration as

$$n_s(x,t) = n_{s0}\int f_s(x,v,t)\, dv \tag{2}$$

and are coupled through Poisson's equation

$$\frac{\partial^2\phi(x,t)}{\partial x^2} = \frac{e}{\epsilon_0}\left[n_e(x,t) - n_i(x,t) + Z_d n_d(x,t)\right]. \tag{3}$$

The equilibrium values $n_{s0}$ are assumed to satisfy the quasi-neutrality condition

$$n_{e0} - n_{i0} + Z_d n_{d0} = 0, \tag{4}$$

at the initial time step of our simulation.

For the sake of simplicity, the above system of equations has been cast in dimensionless form (rescaled) as follows. Space and time are normalized by $\lambda_{Di}$ and $\omega_{pi}^{-1}$, respectively, where $\omega_{pi} = [n_{i0}e^2/(m_i\epsilon_0)]^{1/2}$ denotes the ion plasma frequency and $\lambda_{Di} = [(\epsilon_0 k_B T_i)/(n_{i0}e^2)]^{(1/2)}$ is the characteristic ion Debye length. The velocity variable $v$ has been scaled by the ion thermal speed $v_{th_i} = (k_B T_i/m_i)^{1/2}$, while the electric field and the electric potential have been scaled by $k_B T_i/(e\lambda_{Di})$ and $k_B T_i/e$, respectively, (here $k_B$ is Boltzmann's constant). The densities of the three species are normalized by $n_{i0}$.

The scaled (dimensionless) Vlasov–Poisson system of equations forming the basis of our study reads

$$\frac{\partial f_e(x,v,t)}{\partial t} + v\frac{\partial f_e(x,v,t)}{\partial x} - \frac{m_i}{m_e}E(x,t)\,\frac{\partial f_e(x,v,t)}{\partial v} = 0, \tag{5}$$

$$\frac{\partial f_i(x,v,t)}{\partial t} + v\frac{\partial f_i(x,v,t)}{\partial x} + E(x,t)\,\frac{\partial f_i(x,v,t)}{\partial v} = 0, \tag{6}$$

$$\frac{\partial f_d(x,v,t)}{\partial t} + v\frac{\partial f_d(x,v,t)}{\partial x} - Z_d\frac{m_i}{m_d}E(x,t)\,\frac{\partial f_d(x,v,t)}{\partial v} = 0, \tag{7}$$

and

$$\frac{\partial^2\phi(x,t)}{\partial x^2} = n_e(x,t) + n_d(x,t) - n_i(x,t). \tag{8}$$

The normalized density functions read

$$n_e(x,t) = \sigma\int f_e(x,v,t)dv, \tag{9}$$

$$n_i(x,t) = \int f_i(x,v,t)dv, \tag{10}$$

and

$$n_d(x,t) = \delta\int f_d(x,v,t)dv. \tag{11}$$

In the above relations, we have defined the *Havnes parameter*[27,28] $\delta = \frac{Z_d n_{d0}}{n_{i0}}$, which represents the scaled charge density of the dust particles (note that $\delta$ vanishes in the absence of dust) and the scaled electron density at equilibrium

$\sigma = \frac{n_{e0}}{n_{i0}}$. The latter two parameters are related to each other via the scaled quasi-neutrality equation

$$\sigma = 1 - \delta, \tag{12}$$

implying overall charge neutrality at equilibrium; cf. (4).

Our numerical procedure is as follows. At each time step, the distribution functions are calculated from kinetic equations (5)–(7). Then, the number density of each plasma species is obtained by integration of the distribution function over the velocity range, based on Eqs. (9)–(11). Feeding the corresponding density values into Poisson's equation (8), the electric field is obtained. The instantaneous electric field is then input in the Vlasov equations and the cycle recommences, so that the next step distribution functions and density values are obtained. This cycle is iterated, and the results are retained at every step. Energy preservation is meticulously tested and, indeed, confirmed throughout the procedure.

A Maxwellian state at equilibrium is assumed for all species. In order to excite ion acoustic waves, a small periodic perturbation is added to the initial condition for the ions, i.e., at time $t = 0$

$$f_e(t=0) = \left(\frac{1}{2\pi}\right)^{1/2} \left(\frac{m_e}{m_i}\frac{T_i}{T_e}\right)^{1/2} \exp^{-\left(\frac{m_e T_i}{m_i T_e}\right)}, \tag{13}$$

$$f_i(t=0) = \left(\frac{1}{2\pi}\right)^{1/2} \exp^{-v^2/2}\left[1 + \alpha\cos\left(\frac{2\pi}{\lambda}x\right)\right], \tag{14}$$

and

$$f_d(t=0) = \delta\int\left(\frac{1}{2\pi}\right)^{1/2} \left(\frac{m_d}{m_i}\frac{T_i}{T_d}\right)^{1/2} \exp^{-\left(\frac{m_d T_i}{m_i T_d}\right)\frac{v^2}{2}}. \tag{15}$$

Note that an initial disturbance was imposed on the ions, in order to trigger the anticipated excitation, whose strength is denoted by the parameter $\alpha$ appearing in (14). For the sake of simplicity, we shall set $\theta = T_e/T_i$ in the following:

The constant parameters which remain fixed through all of our simulations are: $m_d/m_i = 10^5$, $m_i/m_e = 10^2$, $T_i/T_d = 400$, $Z_d = 1000$, time step $dt = 0.01$, $\alpha = 0.05$, and $L = \lambda = 5\pi$, where L is the length of the simulation box and $\lambda$ is the initial perturbation wavelength. The values of two other parameters, namely $\theta$ and $\delta$, were modified between successive simulations. However, these values were fed into each simulation at the initial step and remained intact through it, as rigid constants. We have considered a two-dimensional phase space with one spatial and one velocity axis. The phase space grid ($N_x$, $N_v$) size is (100, 2500). We have introduced four phase points per cell, randomly chosen inside each cell to avoid the aforementioned recurrence effect, at the initial step, therefore each simulation involves of $10^6$ phase points.

## III. RESULTS AND DISCUSSION

### A. BGK modes in electron-ion plasmas

We shall start by focusing our study on exciting ion-acoustic excitations in isothermal electron-ion plasma (i.e., setting $\delta = 0$ in the model described above). In order to excite IA waves, a periodic perturbation is imposed on the ion distribution function, given by Eq. (14) with $\alpha = 0.05$.

By increasing the electron-to-ion temperature ratio ($\theta$), Landau damping becomes strongly nonlinear and BGK modes occur, as seen in Figure 1 (while the value of $\alpha$ remains unchanged). In the case of linear Landau damping, parallel filamentation happens in phase space around the phase velocity of the wave; see Figure 2. However, for nonlinear Landau damping and the associated BGK modes, we observe the formation around the phase velocity of more complicated vortex structures which, as far as our study is considered, appear to be stable; see Figure 3.

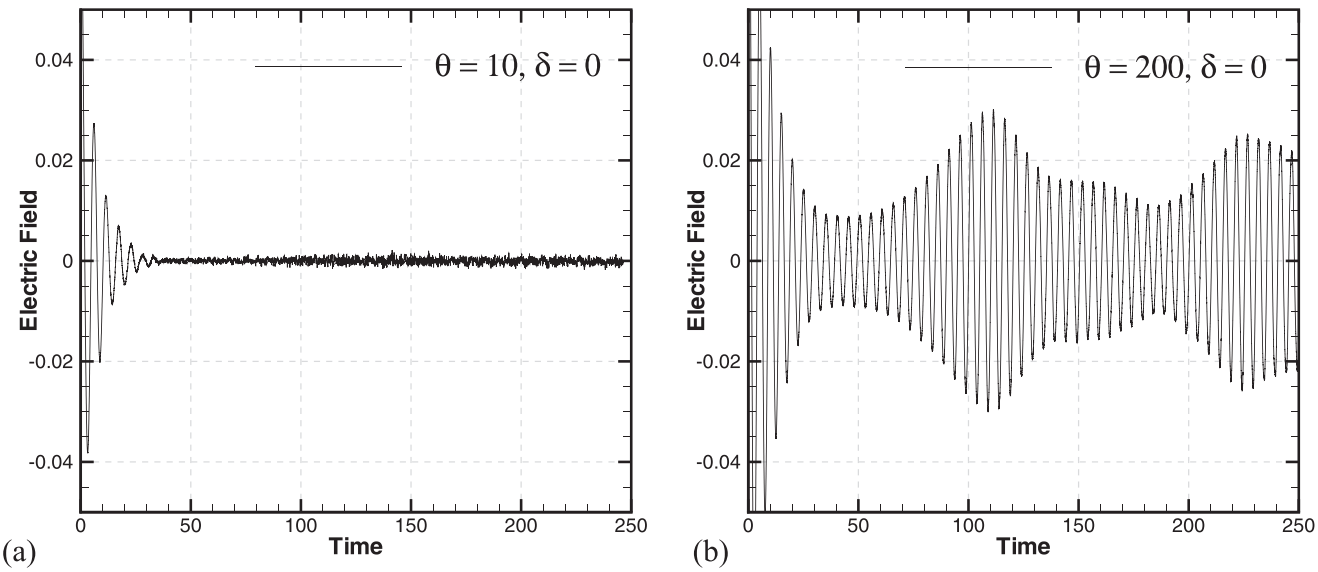


FIG. 1. Electric field evolution versus time (normalized by $\omega_{pi}^{-1}$): (a) For values of $\theta$ sufficiently low, linear Landau damping occurs; (b) by increasing $\theta$, nonlinear Landau damping emerges and BGK modes appear. The figure shows the first two peaks of the E-field associated with BGK modes, the first one appearing around $t = 120\,\omega_{pi}^{-1}$ and the second one around $t = 230\,\omega_{pi}^{-1}$.

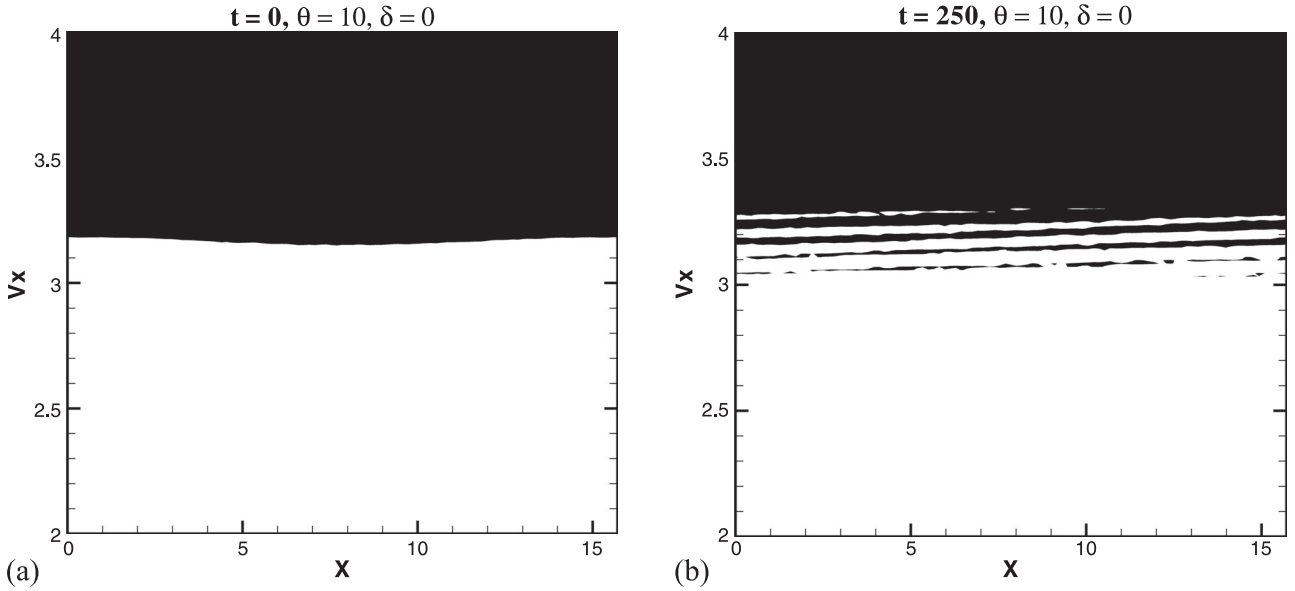


FIG. 2. The phase space portrait of the ion distribution function near the ion-acoustic phase velocity is depicted. The plots show: (a) The initial distribution function (the white/black colored regions, respectively, represent particles with velocities below/above the phase velocity; (b) the distribution function at time $t = 250\,\omega_{pi}^{-1}$, for $\delta = 0$ and $\theta = 10$. Simple parallel filamentation appears in the vicinity of the phase velocity.

In Fig. 4, we have depicted the effect of the temperature ratio ($\theta$) on the amplitude of the E-field, associated with the observed BGK modes. This dependence is intuitively expected. As a matter of fact, the value of the electron-to-ion temperature ratio $\theta$ obviously affects the shape of the distribution function, and, in particular, its slope in the vicinity of the phase velocity (as a matter of fact, the relative slope of the ion distribution function in comparison to the electron distribution function). This should lead to a change in the number of trapped particles, resulting in a modification of the distribution function vortex size in phase space; see Fig. 3 above. Since the phase-space distribution (i.e., the vortex size, here) controls the amplitude of the electric field associated with the BGK modes, it is expected that the electron-to-ion temperature ratio ($\theta$) affects in turn the amplitude of BGK modes.

Another important aspect of BGK modes is the characteristic time scale of fluctuation, to be referred to as $\tau_{trap}$, or the *trapping time*. As evident in Fig. 5, increasing the temperature ratio of electrons over ions bears a considerable effect on the time scale of BGK modes, on one hand, and results in a (nearly exponential) decrease of the trapping-related time scale $\tau_{trap}$, on the other.

As discussed above, the generation of BGK modes is associated with the occurrence of rotating phase-space vortices in phase space; cf. Fig. 3. Accordingly, it is intuitively expected that the characteristics of the observed structures (e.g., time evolution scale, amplitude) should depend on the time periodicity and on the size of the associated vortex, respectively. Figs. 4 and 5 suggest that, by increasing the electron-to-ion temperature ratio, the temporal period of the vortex decreases, while its size increases. In other words, according to our observations, larger phase space vortices rotate faster.

In earlier studies, it has been shown that $\tau_{trap}$ depends on the strength of the perturbation,[10] viz., on $\alpha$ in our model, but the new element here is that it is shown that it depends on parameters like $\theta$ as well. The BGK structure characteristics, namely, the trapping time scale $\tau_{trap}$ and the amplitude $A$, seem to have an exponential dependence on $\theta$, and, as discussed earlier, these also depend on the vortex size. We may postulate, qualitatively, that these vortices have an exponential dependence on $\theta$. A more detailed analysis reveals that the curves can be approximated as $f(\theta) = C[1 - \exp(-a\theta)]$, in which $C$ is a constant with value around $\simeq 0.032$. The value of $a$ is 0.016, 0.03, and 0.15 for $\delta$ equal to 0, 0.5, and 0.9, respectively. As for Fig. 5, a careful numerical fitting shows that the data therein follow a functional form $f(\theta) = D[1 - \exp(-b\theta)]^{-1}$, in which $D$ is constant, around $\simeq 105.5$ in our simulation. The parameter $b$ takes the values: 0.025, 0.064, and 0.25 for $\delta$ equals 0, 0.5, and 0.9, respectively.

### B. BGK modes in dusty plasmas

In this part, we shall focus on BGK modes formed in the presence of dust particles, i.e., DBGK modes.[14] We shall investigate their dependence on two parameters, namely, the electron-to-ion temperature ratio $\theta$ and the normalized dust charge density $\delta$. Two distinct features of these modes will be considered: The saturation level of the electric field amplitude (here the first peak of BGK modes will be focused upon) and the time period of the amplitude fluctuation (here, interpreted as the time of appearance of the first amplitude peak).

The dependence of the amplitude on the electron-to-ion temperature ratio ($\theta$), on one hand, and the normalized dust charge density ($\delta$), on the other, is shown in Figure 6. As we

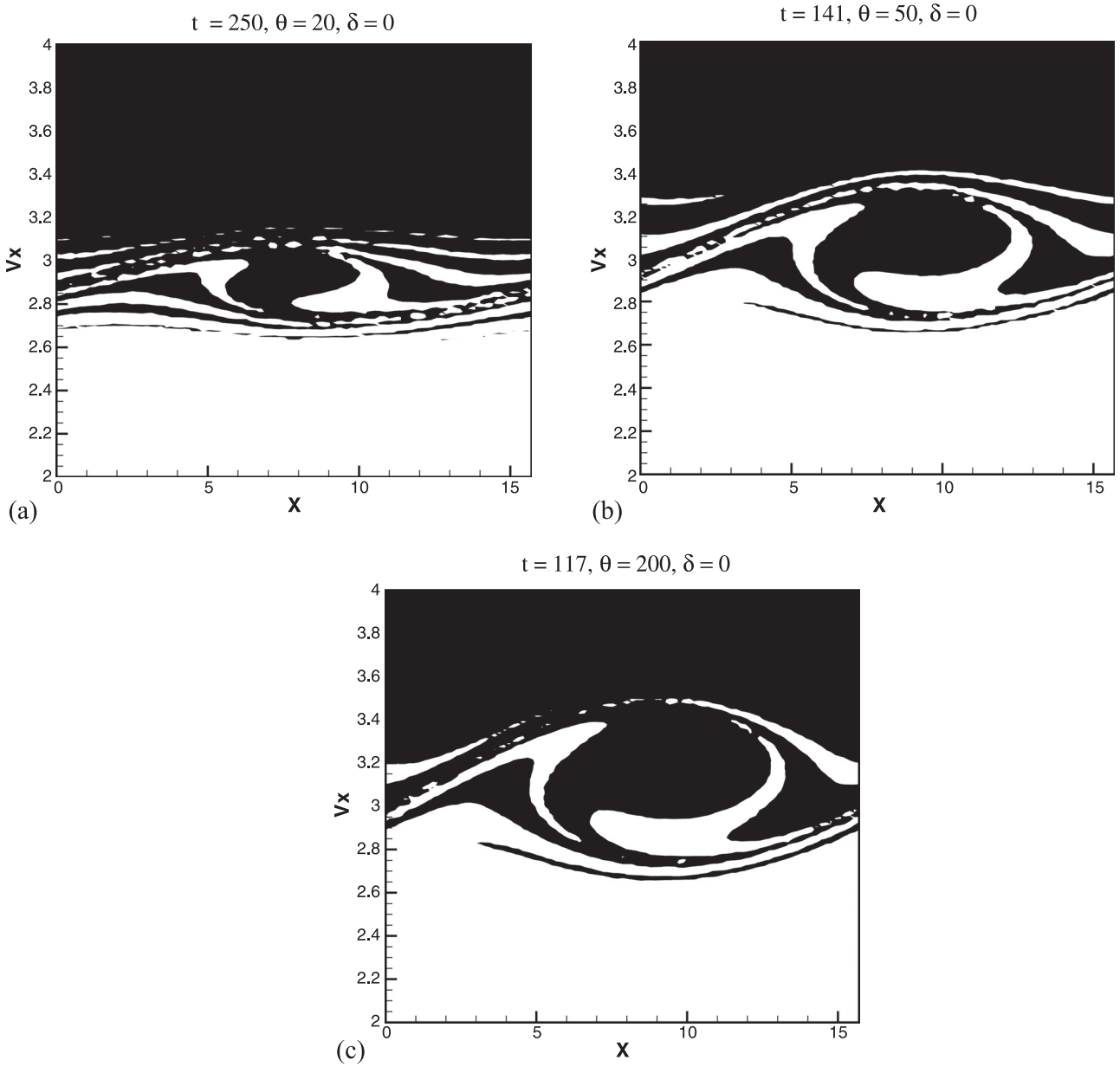


FIG. 3. A phase-space vortex is depicted, for different values of the electron-to-ion temperature ratio $\theta$. Such vortices are responsible for the generation of BGK modes on the ion-acoustic range. Note that the vortex size increases with $\theta$ at the time when the electric field envelope reaches its first peak. The parameter values in these plots are: (a) $\delta = 0,\ \theta = 20$, at time $t = 250\,\omega_{pi}^{-1}$; (b) $\delta = 0,\ \theta = 50$, at time $t = 141\,\omega_{pi}^{-1}$; and (c) $\delta = 0\,, \theta = 200$, at time $t = 117\omega_{pi}^{-1}$.

see in that plot, an increase in the normalized charge density of the dust particles $\delta$ results in a higher amplitude. Let us point out that, as intuitively expected, all three curves (drawn for different $\theta$) tend to the same asymptotic value (0.035) for $\delta \to 1$ (representing the "dust-ion" plasma limit, accounting for complete electron depletion).

Figure 7 represents the (practically linear) dependence of the trapping time $\tau_{trap}$ on the normalized dust charge density ($\delta$). Three different lines are depicted, for different values of $\theta$, which reach the same point $\tau_{trap} = D = 105.5$ around $\delta \simeq 1$.

The trend in both of the latter two diagrams appears to be almost linear. In fact, it can be shown in Fig. 6 that the curves follow the trend $y = a\ (x - 1) + C$. Here, $C$ is a parameter with value: 0.035, and $a$ is 0.02, 0.025, and 0.007, for $\theta = 30$, 50, and 100, respectively. For Fig. 7, the relation is $y = b\ (1 - x) + D$, in which $D \simeq 105.5$ and $b$ is approximately equal to 65, 35, and 15, for $\theta$ equal to 30, 50, and 100, respectively.

### C. Comparison with theoretical results

In order to interpret the observed characteristics of BGK modes in a dusty plasma, the method proposed by Bernstein *et al.*[1,29] will be employed. According to that method, the stationary state of the plasma is considered; in other words, the problem will be solved in the moving wave frame (moving at the phase speed).

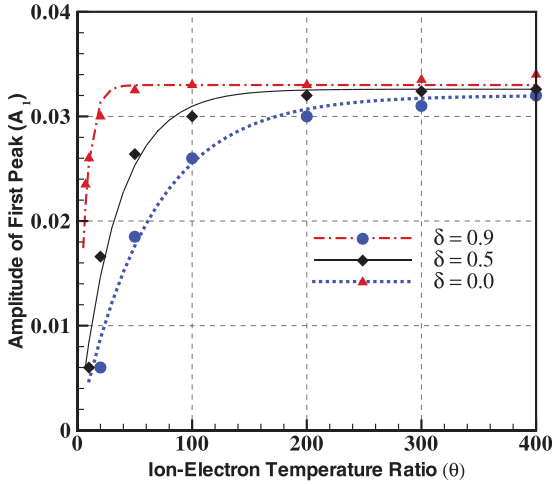


FIG. 4. The exponential dependence of the amplitude of BGK modes on the electron-to-ion temperature ratio $\theta$ is depicted, for different values of $\delta$. As $\theta$ increases, the localized E-field amplitude follows an exponential increase and asymptotically reaches a certain level of saturation, which here is about 0.035. This actually implies that by increasing $\theta$, the size of the phase-space vortex becomes bigger, since $A_1$ is directly related to the size of the phase-space vortex. The amplitude of the first peak is considered in these plots.

Recalling that all three elements are characterized by a Maxwellian distribution function at equilibrium, Poisson's equation after linearization and normalization reads

$$\frac{\partial^2 \varphi_1(x)}{\partial x^2} + \left(1 + \frac{1-\delta}{\theta} + \delta\frac{T_i}{T_d}\right)\varphi_1(x) = 0\,. \tag{16}$$

The latter relation represents harmonic oscillations, provided that

$$k^2 = 1 + \frac{1-\delta}{\theta} + \delta\frac{T_i}{T_d} > 0, \tag{17}$$

which is always satisfied in our case (recall that $0 \le \delta \le 1$).

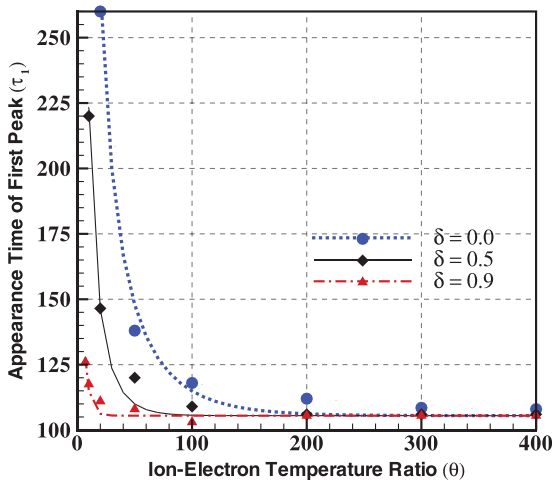


FIG. 5. The exponential dependence of the trapping time $\tau_{trap}$ on the electron-to-ion temperature ratio $\theta$ is depicted, for different $\delta$. Rapid decrease can be observed in $\tau_{trap}$ by increasing the value of $\theta$. However, for $\theta > 90$, the $\tau_{trap}$ reaches its saturation level and stops dropping. This saturation level is around 100.

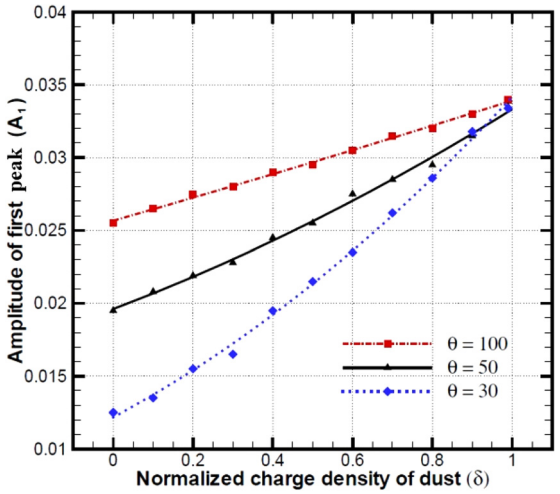


FIG. 6. The relationship between the amplitude of BGK modes $A_1$ and the normalized charge density of dust particles $\delta$ is depicted, for three different values of $\theta$. An increase in $\delta$ results in a practically linear increase in the amplitude. All of the three different curves for different $\theta$ tend to the same value (0.035) for $\delta \to 1$.

The harmonic solution of (16) reads

$$\phi = \phi_0 \sin(kx + \beta), \tag{18}$$

where $\phi_0$ and $\beta$ are arbitrary constants (and $k$ was defined previously). The resulting electric field is $E = d\phi(x)/dx = k\phi_0 \cos(kx + \beta)$, implying that the maximum electric field varies as

$$E_{max} \sim \left(1 + \frac{1-\delta}{\theta} + \delta\frac{T_i}{T_d}\right)^{1/2}. \tag{19}$$

In Fig. 8, a comparison between the theoretical and the observed simulation results is shown, showing good agreement with each other.

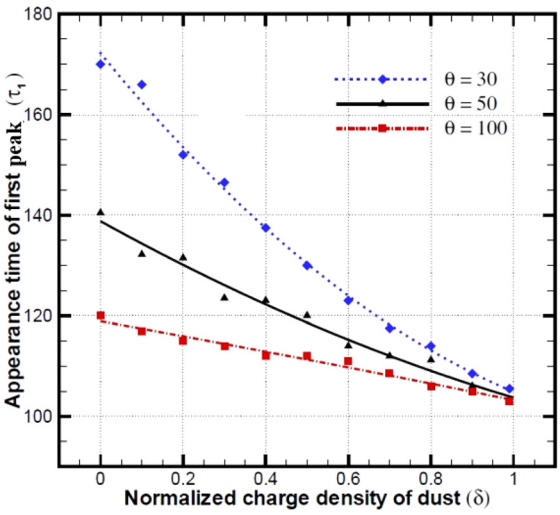


FIG. 7. The relationship between the trapping time $\tau_{trap}$ of BGK modes and the normalized charge density of dust particles $\delta$ is depicted, for different value of $\theta$.

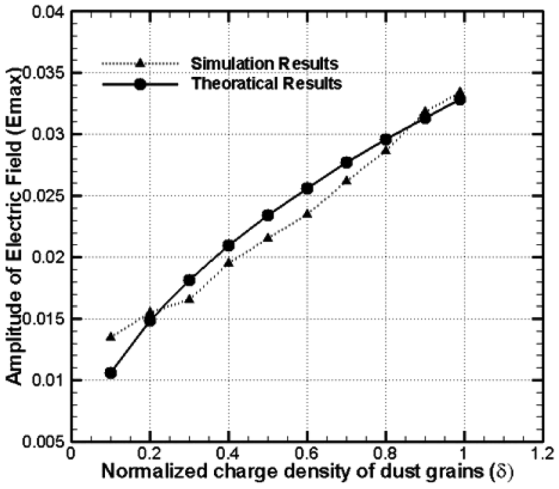


FIG. 8. The results of our theoretical approach are compared to the simulation outcome, for the electric field amplitude. We observe a fairly good agreement between the two curves.

## IV. CONCLUSIONS

We have investigated the characteristics of BGK modes associated with ionic-scale electrostatic excitations via a series of kinetic simulations of a two- (electron-ion) and three- (electron-ion-dust) component plasma. A fully kinetic algorithm has been adopted, i.e., by treating all plasma components via a Vlasov equation.

We have focused, in particular, on the characteristics of BGK-type kinetic structures—namely, the electric field amplitude and the periodicity—and have observed how these depend on the relevant plasma-compositional parameters, i.e., the electron-to-ion temperature ratio and the dust concentration. Summarizing our qualitative observations, we have seen that the measurable characteristics of the BGK modes show an exponential dependence on the electron-to-ion temperature ratio $\theta$, while on the other hand, they depend on the dust charge density (Havnes) parameter $\delta$, this relationship is practically linear.

The amplitude of BGK modes directly depends on the size of the vortex appearing in the ion distribution in phase space, hence their dependence on various parameters essentially reflects their effect on the characteristics (size, rotation speed) of the associated phase space vortices at the first place.

## ACKNOWLEDGMENTS

S. M. Hosseini Jenab is grateful to Dr. Agha Hoseini, Dr. Abasi, and Dr. Sharam Motaghiani for their help and support. He is also grateful to Amirkabir University of Technology. I.K. gratefully acknowledges funding from the UK EPSRC (Engineering and Physical Science Research Council) via Grant No. EP/I031766/1.

[1]I. B. Bernstein, J. M. Greene, and M. D. Kruskal, Phys. Rev. **108**, 546 (1957).
[2]J. P. Lynov, P. Michelsen, H. L. Pecseli, J. J. Rasmussen, K. S. Saeki, and V. A. Turikov, Phys. Scr. **20**, 328 (1979).
[3]K. Saeki, P. Michelsen, H. L. Pecseli, and J. J. Rasmussen, Phys. Rev. Lett. **42**, 501 (1979).
[4]M. Temerin, K. Cerny, W. Lotko, and F. S. Mozer, Phys. Rev. Lett. **48**, 1175 (1982).
[5]H. Matsumoto, H. Kojima, T. Miyatake, Y. Omura, M. Okada, I. Nagano, and M. Tsutsui, Geophys. Res. Lett. **21**, 2915, doi:10.1029/94GL01284 (1994).
[6]R. E. Ergun, C. W. Carlson, J. P. McFadden, F. S. Mozer, L. Muschietti, I. Roth, and R. J. Strangeway, Phys. Rev. Lett. **81**, 826 (1998).
[7]J. Franz, P. M. Kintner, and J. S. Pickett, Geophys. Res. Lett. **25**, 1277, doi:10.1029/98GL50870 (1998).
[8]C. A. Cattell, J. Dombeck, J. R. Wygnant, M. K. Hudson, F. S. Mozer, M. A. Temerin, W. K. Peterson, C. A. Kletzing, and C. T. Russell, Geophys. Res. Lett. **26**, 425, doi:10.1029/1998GL900304 (1999).
[9]A. Mangeney, C. Salem, C. Lacombe, J.-L. Bougeret, C. Perche, R. Manning, P. J. Kellogg, K. Goetz, S. J. Monson, and J.-M. Bosqued, Ann. Geophys. **17**, 307 (1999).
[10]T. M. O'Neil, Phys. Fluids **8**, 2255 (1965).
[11]F. F. Chen, *Introduction to Plasma Physics and Controlled Fusion: Plasma Physics* (Plenum Press, New York, 1984).
[12]A. Luque and H. Schamel, Phys. Rep. **415**(56), 261 (2005).
[13]P. K. Shukla and V. P. Silin, Phys. Scr. **45**, 508 (1992).
[14]M. Tribeche, R. Hamdi, and T. H. Zerguini, Phys. Plasmas **7**, 4013 (2000).
[15]A. A. Vlasov, J. Exp. Theor. Phys. **8**, 291 (1938); A. Vlasov, Sov. Phys. Usp. **10**, 721 (1968).
[16]C. Z. Cheng and G. Knorr, J. Comput. Phys. **22**, 330 (1976).
[17]R. B. Horne and M. P. Freeman, J. Comput. Phys. **171**, 182 (2001).
[18]T. Utsumi, T. Kunugi, and J. Koga, Comput. Phys. Commun. **108**, 159 (1998).
[19]B. Eliasson, J. Comput. Phys. **225**, 1508 (2007).
[20]H. Abbasi, M. H. Jenab, and H. H. Pajouh, Phys. Rev. E **84**, 036702 (2011).
[21]F. Kazeminezhad, S. Kuhn, and A. Tavakoli, Phys. Rev. E **67**, 026704 (2003).
[22]G. Manfredi, Phys. Rev. Lett. **79**, 2815 (1997).
[23]M. B. Isichenko, Phys. Rev. Lett. **78**, 2369 (1997).
[24]V. V. Demchenko, N. M. El-Siragy, and A. M. Hussein, Phys. Lett. A **44**(3), 193 (1973).
[25]S. M. H. Jenab, I. Kourakis, and H. Abbasi, Phys. Plasmas **18**, 073703 (2011).
[26]G. Manfredi and P. Bertrand, Phys. Plasmas **7**, 2425 (2000).
[27]P. K. Shukla and A. A. Mamun, *Introduction to Dusty Plasma Physics* (Institute of Physics Publishing, Bristol, Philadelphia, 2002).
[28]*NRL Plasma Formulary*, Naval Research Laboratory, Washington, D.C., 2013.
[29]H. Houili, M. Tribeche, and K. Aoutou, Phys. Plasmas **9**, 4385 (2002).